

SCIENTIFIC REPORTS



OPEN

Nano-Antennas Based on Silicon-Gold Nanostructures

A. Kucherik¹, S. Kutrovskaya^{2,1}, A. Osipov¹, M. Gerke¹, I. Chestnov^{2,1}, S. Arakelian¹, A. S. Shalin³, A. B. Evlyukhin^{3,4} & A. V. Kavokin²

Received: 9 October 2018

Accepted: 28 November 2018

Published online: 23 January 2019

We experimentally realize nano-antennas based on hybrid silicon-gold nanoparticles (NPs). The silicon particles covered by clusters of small metal NPs are fabricated from a liquid phase under the effect of the laser irradiation. The complex nanoclusters containing both Si and Au components provide the enhancement of the near-field intensity and the resonant light scattering associated with excitation of multipole resonances in NPs. A strong sensitivity of the resonant light absorption to the hybrid particle size and material parameters is experimentally documented and theoretically discussed. The results demonstrate a high potentiality of the hybrid NPs for the realization of functional optical devices and metasurfaces.

Light scattering by micro- and nano-particles is at the origin of a rich variety of non-trivial optical effects that pave the way to multiple photonic applications. In this context, one of the most promising applications of NPs is for fabrication of nano-antennas able to transfer the electromagnetic field energy from near-field to far-field and vice versa on spatial scale of a few nanometers. One of the important challenges on the way to the optimization of such nano-antennas is the reduction of Ohmic losses. The Ohmic losses tend to be very high at the optical frequencies in metallic structures usually employed in nano-antennas¹. Optical absorption and high Ohmic losses result in a significant heating that negatively affects the performance of these nano-antennas. On the other hand, certain dielectric and semiconductor nanostructures are characterized by much lower losses in the visible range that makes them suitable candidates for nano-antenna applications. In particular, it has been theoretically predicted² and experimentally demonstrated that silicon NPs of a diameter of 100 and 200 nm possess well-resolved dipole resonances in the visible range^{3,4}. The interplay between electric and magnetic multipole resonances in silicon NPs leads to a number of new effects such as the self-focusing of radiation, suppression of the back scattering etc⁵.

Combining the characteristics of noble metal and silicon NPs, one can potentially take advantage of the specific optical properties of both of them. In this context, hybrid silicon-metal NPs are especially promising as they allow for tailoring optical properties, plasmon resonances, electric and magnetic response functions.

Our work is aimed at the experimental demonstration of such tailoring and the enhancement of the near field emission of silicon NPs by covering them by small-size gold NPs. Golden shells trigger a remarkable nano-antenna effect that strongly affects the near field emission of silicon. We have already presented the suitable method on the formation of hybrid gold-silicon NPs with an on-demand size by laser irradiation of colloidal solutions⁶. The increase of the magnitude of NPs near field intensity is theoretically described in terms of multipole interaction in hybrid clusters triggered by the presence of golden nanoparticles. The remarkable resonant scattering properties of NPs are a consequence of the multipole effect as well.

Results

The Preparation of Colloidal Systems Based on Nps. We have used the CW-laser ablation for creation of liquid colloidal systems containing Si or gold NPs and the additional pulse laser action to induce the hybrid cluster formation as described in refs^{7,8}. The average size of synthesized NPs and its dispersion were tuned by variation of the parameters of laser irradiation⁸ and probed by the dynamic light scattering. Hereafter we discuss the possibility of using of spherical silicon NPs with diameters of 100 nm and 200 nm as cores of hybrid clusters, in particular. This is because these NPs are expected to show spectrally separated dipole resonances in the visible

¹Department of Physics and applied mathematics, Stoletov Vladimir State University, 600000, Gor'kii street 87, Vladimir, Russia. ²Westlake University, 18 Shilongshan Road, 310000, Cloud Town, Xihu District, Hangzhou, China. ³ITMO University, 49 Kronversky Ave., 197101, St. Petersburg, Russia. ⁴Moscow Institute of Physics and Technology, 9 Institutsky Lane, Dolgoprudny, 141700, Russia. Correspondence and requests for materials should be addressed to A.K. (email: kucherik@vlsu.ru)

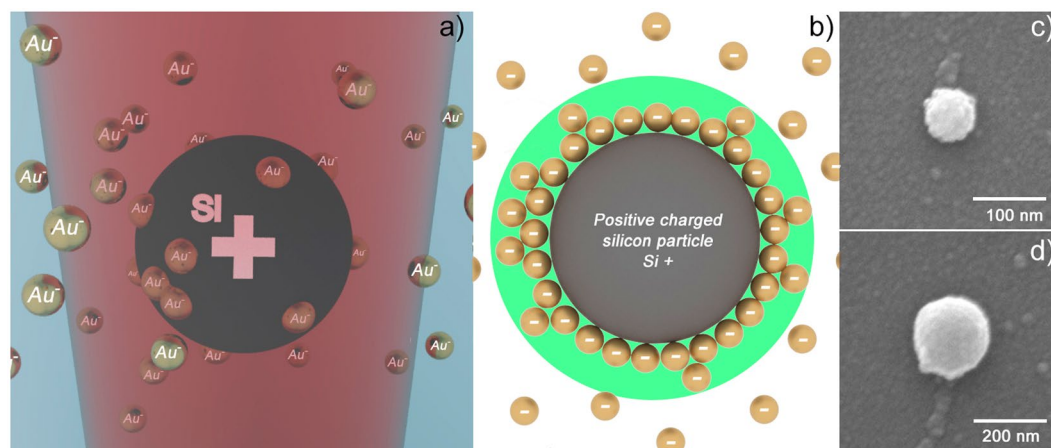


Figure 1. From left to right: the schematic image of the hybrid NPs formation under effect of the laser action on a liquid system consisting of Si and Au NPs (a); the scheme of the electrical double layer formation near the Si NP (b); the SEM-images of hybrid clusters composed by central silicon parts having a diameter of 100 nm and 200 nm and 10 nm gold nanoparticles covering the central silicon NP (c,d).

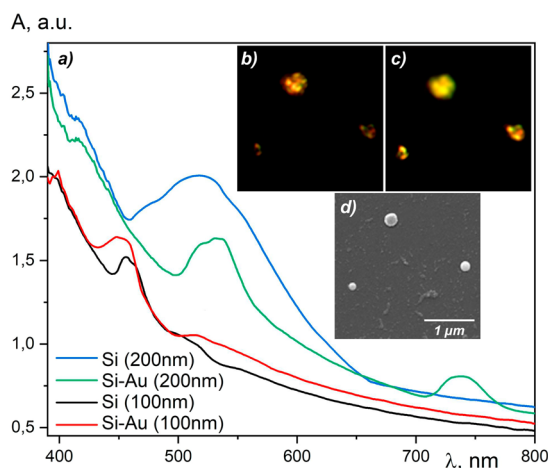


Figure 2. The absorption spectra (a) of liquid systems based on Si NPs of 100 nm (black curve) or 200 nm (blue curve) sizes, hybrid Au-Si nanoclusters with the silicon core of a diameter of 100 nm (red) and 200 nm (green curves); the inset subtracting a combined images (only the scattered light is collected) of the deposited hybrid gold-silicon nanoclusters for different illumination intensities: the white light intensity increases from 1000 lm (b) to 2000 lm (c). The SEM images of hybrid Si-Au NPs (d).

range. We argue that an uneven gold covering including Au particles of 10 nm should result in the increase of dipole-dipole interactions in the nanocluster, in general.

The physical mechanism of clusters' formation is as follows (see Fig. 1). The gold NPs produced by laser ablation in liquid using the method described in ref.⁸ are characterized by a shortage of electrons. This shortage is revealed by the z-potential measurement. On the other hand, a colloidal system containing negatively charged NPs exhibits an electrolyte behavior⁹. The additional electrical charge is accumulated on the surfaces of the silicon NPs under the laser illumination. If there is a sufficient concentration of Au particles, their attraction to silicon NPs overcomes the electrostatic repulsion between equally charged NPs so that Si and Au particles start to agglomerate. After electron relaxation owing to the high surface charge density¹⁰, in the peripheral parts of the colloid the electrostatic repulsion is still dominant, so that the NPs are stabilized, and no further cluster growth takes place.

Optical Study of Hybrid Nanoclusters. The initial Si colloidal systems demonstrate a resonant absorption in the spectral range of 450–500 nm for 100 nm NPs and 450–550 nm for 200 nm NPs (see Fig. 2). We detected wide absorption peaks caused by the NP size dispersion in the colloidal solution. Gold nanoparticles demonstrate plasmon resonances with the central wavelength of 523 nm.

After laser irradiation we observed dramatic changes of the optical properties of the colloidal systems. The spectroscopy investigation of the resulted liquid systems allows to identify the difference between absorption

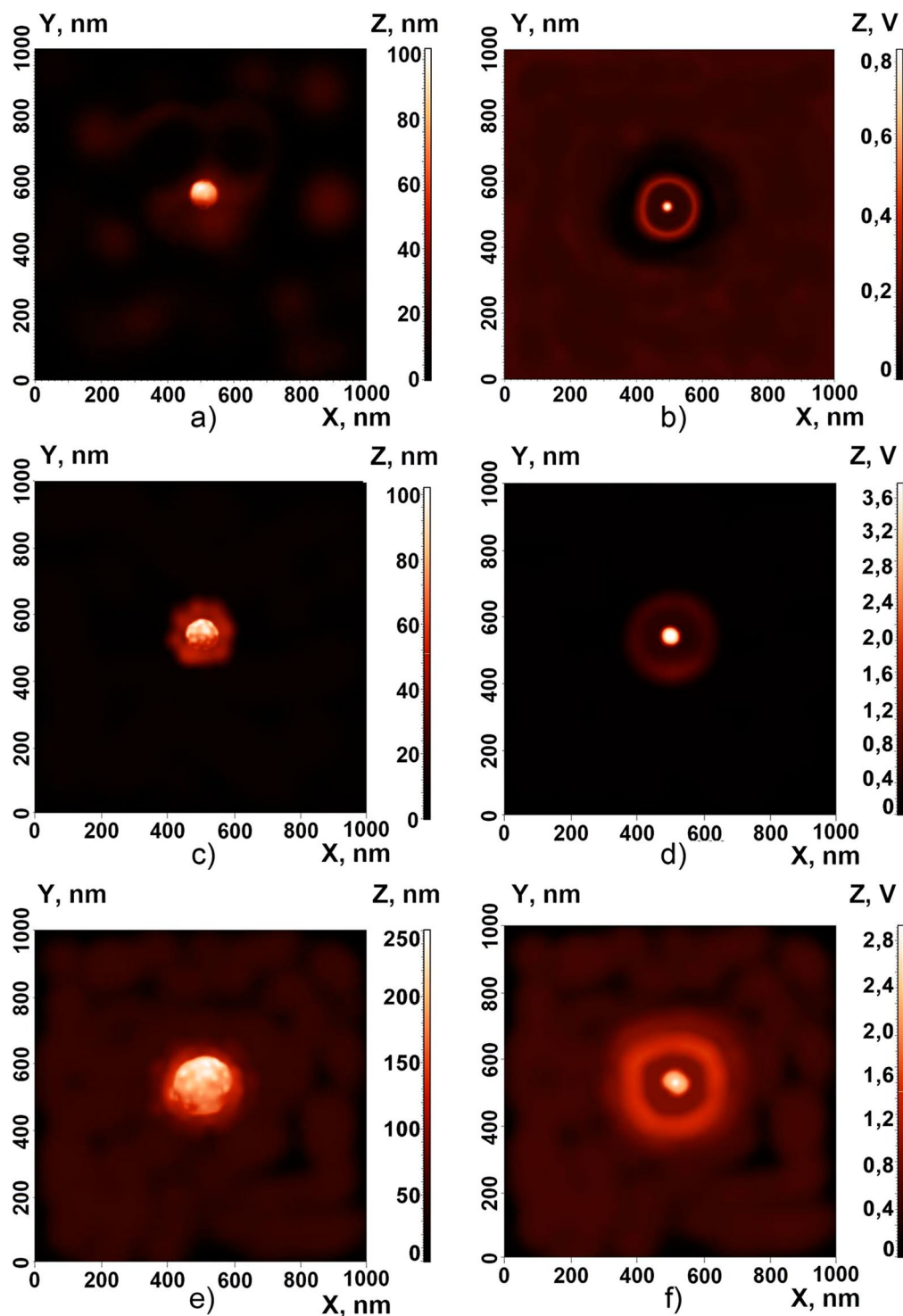


Figure 3. The images made by using atomic-force (a,c,e) and scanning near-field optical (b,d,f) microscopies of the pure Si particle of 100 nm diameter (top panels); 100 nm (medium panels) and 200 nm (bottom panels) Si-Au clusters.

spectra of pure Si NPs and Si-Au cluster systems of the same sizes. This modification is caused by the cluster formation of silicon and gold NPs. The hybrid gold-silicon NPs are characterized by narrow amplitude peaks at about $\lambda \sim 530 \pm 30$ nm and at about $\lambda \sim 740 \pm 30$ nm (for Si-Au (200 nm) in Fig. 2) and by broad peak at about $\lambda \sim 440 \pm 20$ nm and a broad shoulder at about $\lambda \sim 500$ – 600 nm (for Si-Au (100 nm) in Fig. 2). In the single particle approximation the absorption increases for Si-Au case as compared to the reference case of a pure silicon nanoparticle. The theoretical modeling results that are presented below fully reproduces these peculiarities. However, in the case of light scattering on a set of particles in a colloidal system, some more complex optical effects can

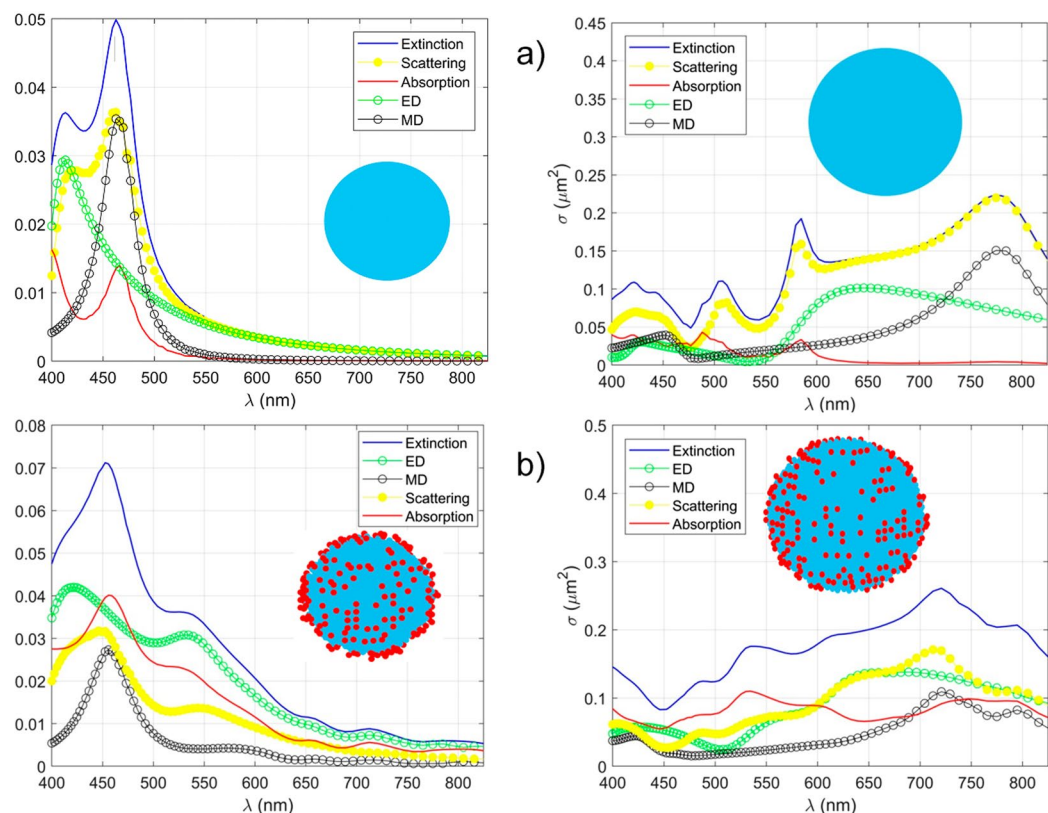


Figure 4. The spectra of the extinction, scattering and absorption cross sections calculated for (a) pure spherical Si-particles, (b) the Si-particles covered by random clusters of Au-particles. The left hand panels correspond to the 100 nm Si-particles, the right hand panels correspond to 200 nm Si-nanoparticles. The diameter of Au-particles is taken equal to 10 nm. The environment medium is air.

be observed. They manifest themselves, in particular, in the strong variation of the absorption coefficient near the frequency of the plasmon resonance. It is important to note that NPs with a diameter of 100 and 200 nm demonstrate the increased absorbance in different spectral ranges. Clearly, the tailoring of hybrid silicon-gold nano-antennas offer a tool for tuning of the dipole resonance frequency in a wide spectral range.

We have deposited NPs using the technology of sputtering small colloidal drops on the solid substrate employing the method described in ref.¹¹. The scanning electron microscopy (SEM) images of several hybrid nanoparticles are shown in Fig. 2, the inserted panel (c). The peculiarity of deposited hybrid nanoparticles was emphasized by the dark-field technique¹². The Mie-scattering in the wide spatial angle on the complex structures due to the illumination of the Si-Au clusters by the unfocused angled beam of a white light has been realized. We observe the changes of the central frequency of resonances from red to yellow spectral ranges (Fig. 2b,c). For the sake of comparison, we deposited clusters consisting of 100 nm and 200 nm Si-Au particles. Interestingly, using different levels of illuminating intensity one can observe various structural features of the nanoparticle clusters (Fig. 2b,c). At the low intensity of illumination one can see the light scattered by inhomogeneities of metal shells. However, this scattered signal vanishes with the increase of the illumination intensity (Fig. 2).

Figure 3 allows one to compare the morphological sizes of clusters revealed by the atomic force microscope (AFM, the left panel) and the distribution of light intensities measured by the scanning near-field optical microscope (SNOM, the right panel). In the case of hybrid clusters the SNOM images are characterized by stronger peaks at the centers of the complex systems surrounded by weaker intensity crowns (see the SNOM profiles at the panels Fig. 3d,f). The increase of the near-field intensity in the hybrid cluster (Fig. 3d) compared to the pure Si NP (Fig. 3b) of the same size is achieved due to the plasmonic enhancement of light in the small metal nanoparticles located at the Si-core surface. It is important to note that the near-field images in Fig. 3 have been observed in the case of illumination at the wavelength of 514 nm that is close to the plasmon resonance of single gold NPs.

Theoretical modelling. In order to interpret the resonant features of the experimental absorption spectra shown in Fig. 2 we applied several theoretical approaches suitable for calculations of the scattering and absorption cross sections of silicon NPs and hybrid silicon-gold NPs. The scattering and absorption spectra of pure spherical Si-particles (Fig. 4a) were obtained in the framework of the Mie theory¹³. Calculations for the Si-particles covered by random clusters of gold nanoparticles (Fig. 4b) were performed within the discrete dipole approximation assuming the presence of random metal-particle clusters (the details of the calculation technique can be found

elsewhere)¹⁴. Dielectric permittivities of Si and Au were taken from¹⁵ and¹⁶, respectively. The results of our simulations are shown in Fig. 4. For a pure Si-particle with a diameter of 100 nm (Fig. 4a, the left hand panel) the resonances of the extinction cross section are governed by the excitation of electric dipole (ED) and magnetic dipole (MD) moments of the NP. The resonant absorption at $\lambda \sim 470$ nm is associated with MD resonances. This explains the experimental data shown in Fig. 2 for Si (100 nm).

If the size of Si-particles increases, the absorption resonances start to be dominated by high-order multipoles. These are the magnetic quadrupole (MQ) and electric quadrupole (EQ) moments for the pure 200 nm Si-particle (see Fig. 4a, the right-hand panel, $\lambda \sim 490$ nm and $\lambda \sim 580$ nm). The overlap between these two resonances corresponds to the experimentally observed broad absorption maximum shown in Fig. 2 for Si (200 nm). Covering Si-particles by small Au-particles we affect the spectral distributions of the resonances (Fig. 4b). In this case, the total absorption cross sections increase, and the resonances become broader as compared to the case of pure Si-particles. For particles with 100 nm Si-cores (Fig. 4b, the left-hand panel) one can see the absorption peak at $\lambda \sim 460$ nm corresponding to MD excitation and a broad shoulder at $\lambda \sim 530$ nm corresponding to the plasmon resonances of Au-NPs. This is in a good agreement with experimental results shown in Fig. 2 for Si-Au (100 nm). The right-hand panel of Fig. 4 shows the calculated spectra of a 200 nm NP. One can see the broad absorption resonance at $\lambda \sim 490$ –590 nm that corresponds to the overlap between the quadrupole resonances of the Si-core and the plasmon resonance of the Au-NP cluster. The absorption increases at $\lambda \sim 750$ nm is due to the combined effect of the MD resonance of Si-core and the plasmon resonances of Au-NP cluster. The calculated spectral dependence of the absorption cross section is very well correlated with experimental observations shown in Fig. 2 for a Si-Au NP of the 100 and 200 nm sizes. Finally, note that the scattering cross sections presented in Fig. 4b have local maxima distributed over the whole considered spectral range. This feature of the scattering spectra is responsible for the different color features of the dark-field images shown in Fig. 2b,c.

Conclusion

We have applied a method of synthesis of hybrid silicon-gold NPs for producing of 100 and 200 nm hybrid clusters whose optical properties are governed by an interplay of the optical responses of the gold and silicon parts. The developed approach provides an efficient tool of control of the size of hybrid nano-antennas that is paramount for tailoring their optical properties. In colloidal solutions containing Si-Au hybrid particles, strong electric and magnetic multipole resonances have been observed. The possibility of a control of near-field intensity by tailoring the Si-Au hybrid NP size is demonstrated. We have applied several theoretical models which qualitatively reproduce the experimental absorption spectral features. The advantages of hybrid nano-particles for nano-antenna applications are caused by a wide complex of electro-optical characteristics. In particular, the hybrid NPs scatter light of the entire visible range, the intensity of scattering and secondary emission in hybrid clusters is much higher than in individual silicon nanoparticles. Also, the excitation of the Mie-resonance in hybrid clusters can be tailored by tuning the concentrations of gold NPs and the size of a silicon core.

References

- Giannini, V., Fernández-Domínguez, A. I., Heck, S. C. & Maier, S. A. Plasmonic nanoantennas: fundamentals and their use in controlling the radiative properties of nanoemitters. *Chem. Rev.* **111**, 3888–3912 (2011).
- Evyukhin, A. B., Reinhardt, C., Seidel, A., Luk'yunchuk, B. S. & Chichkov, B. N. Optical response features of Si-nanoparticle arrays. *Phys. Rev. B.* **82**, 045404 (2010).
- Shi, L., Tuzer, T. U., Fenollosa, R. & Meseguer, F. A New dielectric metamaterial building block with a strong magnetic response in the sub-1.5-micrometer region: silicon colloid nanocavities. *Adv. Mater.* **24**, 5934–5938 (2012).
- Evyukhin, A. B. *et al.* Demonstration of magnetic dipole resonances of dielectric nanospheres in the visible region. *Nano Lett.* **12**, 3749–3755 (2012).
- Kuznetsov, A. I., Miroshnichenko, A. E., Brongersma, M. L., Kivshar, Y. S. & Luk'yanchuk, B. Optically resonant dielectric nanostructures. *Science.* **354**, 2472 (2016).
- Liu, P. *et al.* Fabrication of Si/Au core/shell nanoplasmonic structures with ultrasensitive surface-enhanced raman scattering for monolayer molecule detection. *J. Phys. Chem. C.* **119**, 1234–1246 (2015).
- Kutrovskaya, S. *et al.* The synthesis of hybrid gold-silicon nano particles in a liquid. *Sci. Rep.* **7**, 10284, <https://doi.org/10.1038/s41598-017-09634-y> (2017).
- Arakelyan, S. M. *et al.* Reliable and well-controlled synthesis of noble metal nanoparticles by continuous wave laser ablation in different liquids for deposition of thin films with variable optical properties. *J. Nanopart. Res.* **18**, 155 (2016).
- Cosgrove, T. *Colloid Science Principles, Methods, and Applications*. Hoboken, Wiley-Blackwell (2010).
- López-García, J. J., Aranda-Rascón, M. J. & Horno, J. Electrical double layer around a spherical colloid particle: The excluded volume effect. *J. Colloid Interface Sci.* **316**, 196–201 (2007).
- Antipov, A. A. *et al.* Optical properties of nanostructured gold–silver films formed by precipitation of small colloid drops. *Opt Spectrosc.* **119**, 119–123 (2015).
- Spinelli, P., Verschuuren, M. A. & Polman, A. Broadband omnidirectional antireflection coating based on subwavelength surface Mie resonators. *Nature Commun.* **3**, 692 (2012).
- Bohren, C. F., Huffman, D. R. *Absorption and Scattering of Light by Small Particles*. Weinheim, Wiley-VCH (1998).
- Evyukhin, A. B. *et al.* Influence of metal doping on optical properties of Si nanoparticles. *Optics Commun.* **316**, 56–60 (2014).
- Palik, E. *Handbook of Optical Constant of Solids*. San Diego, Academic Press (1985).
- Johnson, P. B. & Christy, R. W. Optical constants of the noble metals. *Phys. Rev. B.* **6**, 4370 (1972).

Acknowledgements

This work is supported by the Ministry of Science and Higher Education of the Russian Federation (state project no. 16.5592.2017/6.7) and RFBR grants 16-32-60067 mol_a_dk, 17-42-330928 r_a. Multipole decomposition calculations have been supported by the Russian Science Foundation Grant 16-12-10287. It has been performed with a participation of the Innovative Team of International Center for Polaritonics that is supported by Westlake University (Project No. 041020100118).

Author Contributions

A.K. has performed light scattering experiments; S.K. has conceived the work and realized A.F.M. and S.N.O.M. microscopy experiments; A.O. contributed to the laser ablation experiments; M.G. has performed optical absorption measurements; I.C. realized SEM microscopy study; S.A. has realized the single cluster deposition; A.S. contributed to the dark field microscopy of the deposited NPs; A.E. has contributed to the theoretical model; A.V.K. has contributed to the interpretation of the results. A.K. and A.V.K. have written the manuscript.

Additional Information

Competing Interests: The authors declare no competing interests.

Publisher's note: Springer Nature remains neutral with regard to jurisdictional claims in published maps and institutional affiliations.



Open Access This article is licensed under a Creative Commons Attribution 4.0 International License, which permits use, sharing, adaptation, distribution and reproduction in any medium or format, as long as you give appropriate credit to the original author(s) and the source, provide a link to the Creative Commons license, and indicate if changes were made. The images or other third party material in this article are included in the article's Creative Commons license, unless indicated otherwise in a credit line to the material. If material is not included in the article's Creative Commons license and your intended use is not permitted by statutory regulation or exceeds the permitted use, you will need to obtain permission directly from the copyright holder. To view a copy of this license, visit <http://creativecommons.org/licenses/by/4.0/>.

© The Author(s) 2019